

Determination of magnetic anisotropies, interlayer coupling, and magnetization relaxation in FeCoB/Cr/FeCoB

Y. Gong,¹ Z. Cevher,¹ M. Ebrahim,¹ J. Lou,² C. Pettiford,² N. X. Sun,² and Y. H. Ren^{1,a)}

¹*Department of Physics and Astronomy, Hunter College, The City University of New York, 695 Park Avenue, New York, New York 10065, USA*

²*Department of Electrical and Computer Engineering, Northeastern University, 409 Dana Research Center, 360 Huntington Avenue, Boston, Massachusetts 02115, USA*

(Received 14 May 2009; accepted 17 August 2009; published online 24 September 2009)

We studied magnetic anisotropic properties, interlayer coupling, and spin wave relaxation in ten periods of CoFeB/Cr/CoFeB films grown on seed layers of Cu with a Co:Fe:B composition ratio of 2:2:1. The measurements were taken in samples with 50 Å layers of CoFeB using the ferromagnetic resonance technique. The thickness of the Cr interlayers was varied from 4 to 40 Å for understanding the mechanisms of interlayer coupling. We investigated the magnetic anisotropy parameters by rotating the sample with respect to the microwave magnetic field from in plane to perpendicular to the plane. We identify both the acoustic branch and the optical branch in the spin wave resonance spectra. The effective interlayer coupling constant and the out-of-plane anisotropy show an oscillatory change, while the uniaxial in-plane anisotropy increases monotonically with increasing the thickness of the spacing layers. Moreover, we show that the spin wave relaxation can be optimized by adjusting the interlayer exchange interactions. © 2009 American Institute of Physics. [doi:10.1063/1.3225608]

I. INTRODUCTION

Soft magnetic materials have attracted a lot of attention through recent years because of their potential applications in spintronics, magnetic sensors, microwave structures, and high-density magnetic recording devices.^{1–6} Among these, layered film structures such as exchange biased bilayers have been studied extensively. The strong coupling between the ferromagnetic (FM) and antiferromagnetic (AFM) layers has allowed one to introduce effective anisotropies as well as exchange bias in the FM layer.^{7–12} For example, Grimsditch *et al.*¹³ showed that a large magnetic anisotropy can be induced in the Co film deposited on the AFM FeF₂ substrate even well above its Néel temperature. The result is explained by interactions of the ferromagnet with locally ordered regions within the antiferromagnet. Zhou and Chien¹⁴ revealed a large coercivity and a strong surface anisotropy field in Co–Ni/FeMn bilayers. The local field is induced by the FM layer and determines the spin structure of the AFM layer.

Compared with the bilayers, the hybrid sandwich FM/AFM/FM structures have proven to show unique advantages.¹⁵ First, the sandwiched films have a higher effective magnetization, resulting in a higher flux conduction capability and they show excellent magnetic softness with a uniaxial anisotropy field and a low coercivity.¹⁵ The materials provide a unique means to investigate the interfacial interaction and the exchange coupling.¹⁶ Second, the FM/AFM/FM structures can have their magnetic behaviors influenced by layer thickness, crystalline phase growth conditions, and strain between juxtaposed crystalline layers. Such influences affect magnetic ordering temperature, magnetic anisotropy, magnetic axis, and magnetic coupling of

magnetic layers through a nonmagnetic or an AFM layer.^{17–22} Moreover, they are the essential component required to build blocks of the so-called spin valves, which usually generate the giant magnetoresistance and other interesting magnetic properties.^{23–25}

The interlayer interactions between FM layers and between FM and AFM layers seem to be critical for controlling the magnetic properties in multilayer structures. It has been found that in the case of rather thin (from several to tens of angstroms) interlayers, this interaction brings about magnetic ordering of a multilayer structure. Depending on the interlayer thickness, FM or AFM ordering of magnetic moments of neighboring FM layers may be realized. In this context, Planckaert *et al.*²⁶ discussed that the static magnetic ordering may affect the interlayer coupling in the Fe/FeSi/Fe trilayer. Heinrich *et al.*^{27,28} showed that a long-range dynamic interaction is communicated by nonequilibrium spin currents in the Fe/Cu/Fe structure, and the magnetic coupling between the Fe layers changes from FM to AFM as the Cu interlayer thickness increases. The interlayer interactions directly affect the magnetic ordering and the dynamical performance of the multilayer structure.^{16,29,30} Although much progress has been made in the past few years, there are still some fundamental problems regarding the underlying physics of magnetic interactions, exchange couplings, and magnetization relaxations. In particular, little is known about the dynamic magnetic properties of FM/AFM/FM structures, e.g., magnetic anisotropies, interlayer coupling, and the mechanism of magnetization damping, which are of great importance to assess the technological potential of these materials. Because of the high resistivity and relatively high saturation magnetization it can reach, the FeCoB alloys are desired for ultrahigh frequency devices such as future write heads and wireless

^{a)}Electronic mail: yre@hunter.cuny.edu.

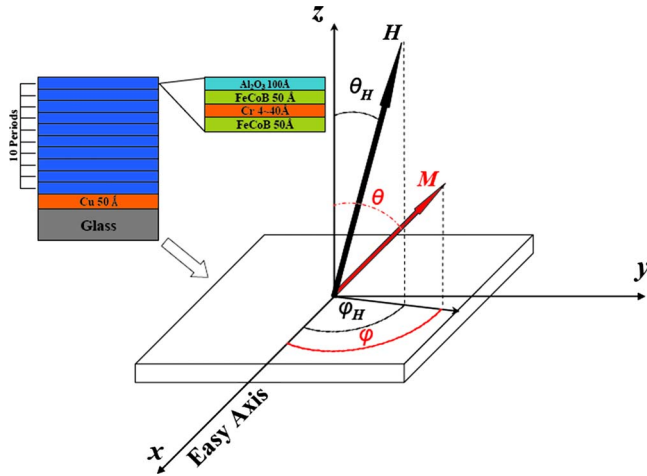


FIG. 1. (Color online) Sample structure and the polar coordinate system used in our measurements. For the in-plane configuration, the applied magnetic field was rotated with respect to the easy axis ($\varphi=0^\circ$) in the sample plane ($\theta=90^\circ$). For the out-of-plane configuration, the applied field was rotated with respect to the perpendicular orientation with $\varphi=0^\circ$.

inductors.³¹ It is fundamentally important to investigate the magnetic dynamical properties of FM/AFM/FM sandwich structures based on FeCoB.

In this work, we used the ferromagnetic resonance (FMR) technique to investigate the magnetic dynamic properties of the FeCoB/Cr/FeCoB multilayer with varying Cr layer thicknesses. The acoustic and optical modes were identified in our FMR spectra. We determined the interlayer coupling constant, the magnetic anisotropies, and the magnetization damping as a function of the Cr layer thickness. The out-of-plane magnetic anisotropy and the magnetization damping show an oscillatory change with increasing interlayer spacing. These behaviors are similar to that of the interlayer coupling constant. We see, however, that the in-plane magnetic anisotropy increases monotonically. Our results suggest that we could use the interlayer coupling between the FM layers as an additional means to optimize the magnetic anisotropy and relaxation parameters in multilayer magnetic structures.

II. EXPERIMENT

Ten periods of the trilayer composed of FeCoB/Cr/FeCoB were deposited on the Cu/glass substrate and coated with the Al_2O_3 layer by dc magnetron sputtering with a base pressure in the order of 10^{-9} Torr. The composition ratio of Co:Fe:B is 2:2:1. The sample structure is shown in the inset of Fig. 1. In order to investigate how the interlayer coupling affects the magnetic dynamical properties, we fixed the thickness of the FM layers at 50 Å and varied the thickness of the Cr layer from 4 to 40 Å. During the deposition procedure, we introduced the uniaxial anisotropy field by applying magnetic field annealing. Magnetic fields, such as coercive fields, exchange coupling fields, etc., were all measured with a vibrating sample magnetometer with an error of 1 Oe. We used a Bruker EMX electron paramagnetic resonance spectrometer to collect the FMR spectra at the X-band of ~ 9.74 GHz. The polar coordinate system in the subsequent discussion is plotted in Fig. 1. The dc magnetic field H was

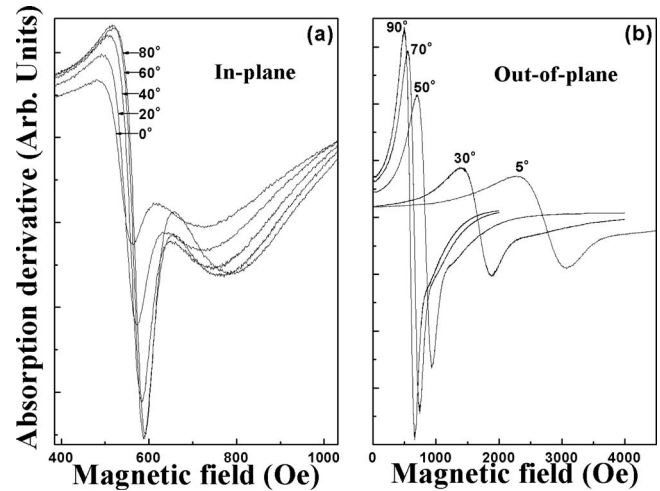


FIG. 2. FMR spectra for various magnetic field orientations in the sample with the 20 Å Cr layers of both (a) the in-plane and (b) the out-of-plane configuration. The asymmetric behavior of the absorption curve is due to the overlap of the acoustic and optical spin wave modes

applied in the horizontal plane, and the microwave magnetic field was along the vertical direction. The samples were placed in a quartz tube inserted in the microwave cavity and rotated with respect to H in an orientation either in the layer plane (change φ) or along the out-of-plane configuration (between the in-plane orientation $\theta=90^\circ$ and the normal to the layer plane $\theta=0^\circ$).

III. RESULTS AND DISCUSSION

A. Spin dynamical acoustic mode and magnetic anisotropy parameters

Figures 2(a) and 2(b) show the FMR spectra in a sample with the 20 Å Cr layers of both the in-plane and the out-of-plane configuration. For the in-plane geometry, the resonant field increases when the applied magnetic field rotates away from the easy axis ($\varphi=0^\circ$). This corresponds to the uniaxial anisotropy field induced by the magnetic field annealing. In contrast, for the out-of-plane configuration, the resonance line shifts a few kilo-oersteds to higher fields as the direction of the magnetic field approaches the film normal, and we observe a significant broadening of the FMR linewidth (as a result, its amplitude decreases). The line shift is induced by the demagnetizing field. For a thin film sample, a macroscopic magnetization could produce a field of $4\pi M$, which points along the perpendicular direction of the sample plane. When we rotate our sample with respect to the applied magnetic field, the equilibrium angle of the magnetization vector depends strongly on the external field value. Therefore, we expect to see a shift of FMR field and an increase in linewidth at an intermediate angle. Moreover, for both configurations, the FMR lines show strong asymmetric behaviors with respect to the base line. The asymmetric behavior of the absorption curve is due to the interlayer coupling of the FM layers. We attribute the feature to the overlap of the in-phase precession and out-of-phase precession resonant modes of the neighboring FM magnetizations, which refer to the acoustic and optical spin wave resonance modes, respectively.

In order to explain the interesting FMR spectra, we introduce the free energy based on a simple trilayer configuration with two FM layer as

$$F = \left(\sum_{i=1}^2 \left\{ -d_i M_i H [\sin \theta_i \sin \theta_H \cos(\varphi_i - \varphi_H) + \cos \theta_i \cos \theta_H] \pm d_i (2\pi M_i^2 - K_{\perp}^i) \sin^2 \theta_i - d_i K_{\parallel}^i \sin^2 \theta_i \cos^2 \varphi_i \right\} \pm J_{\text{inter}} [\sin \theta_1 \cos \theta_2 \cos(\varphi_1 - \varphi_2) + \cos \theta_1 \cos \theta_2] \right), \quad (1)$$

where d_i is the thickness and M_i is the magnetization of each FM layer. H is the applied magnetic field. θ_i , θ_H , φ_i , and φ_H show the orientation of the magnetization and magnetic field in different FM layers with respect to the normal of the sample plane and in-plane easy axis, respectively. K_{\perp} and K_{\parallel} are the out-of-plane uniaxial and in-plane uniaxial anisotropy constants. We also include a bilinear term J_{inter} in the free energy formula for describing the interlayer coupling between the FM layers. We believe that the origin of the interlayer coupling is dominated by the exchange coupling which is an indirect exchange interaction mediated by the conduction electrons of the spacer layer. The interlayer coupling is closely related to the Ruderman–Kittel–Kasuya–Yosida interaction between localized moments mediated by the conduction electrons of a host metal. It is clear that the dipolar interaction does not contribute to the total energy of the system if the magnetization of the film is homogeneous, i.e., $M_1 = M_2$.

We calculate the dispersion relationship of spin wave resonances by applying the equation of resonance frequency of the form³²

$$a\omega^4 + b\omega^2 + c = 0. \quad (2)$$

To solve Eq. (2), we expect two different solutions: $(\omega^{\pm})^2 = (-b \pm \sqrt{b^2 - 4ac})/2a$ that correspond to the in-phase and the out-of-phase precession frequencies (ω^+ and ω^-) of M_1 and M_2 in the two neighboring FM layers, which correspond to the acoustic and optical modes.³³

We simplify the calculation by taking the approximation that $\theta_1 = \theta_2 = \theta$, $\varphi_1 = -\varphi_2 = \varphi_H$, $M_1 = M_2 = M$, $\gamma_1 = \gamma_2$, and $d_1 = d_2$. (The magnetic FeCoB layers are identical.) Then the equations of in-plane and out-of-plane resonance fields for the acoustic mode can be written as

$$\left(\frac{\omega^+}{\gamma} \right)^2 = \left(H_R^a - \frac{2K_{\parallel}}{M} \cos 2\varphi \right) \left(H_R^a + 4\pi M - \frac{2K_{\perp}}{M} + \frac{2K_{\parallel}}{M} \sin^2 \varphi \right), \quad (3)$$

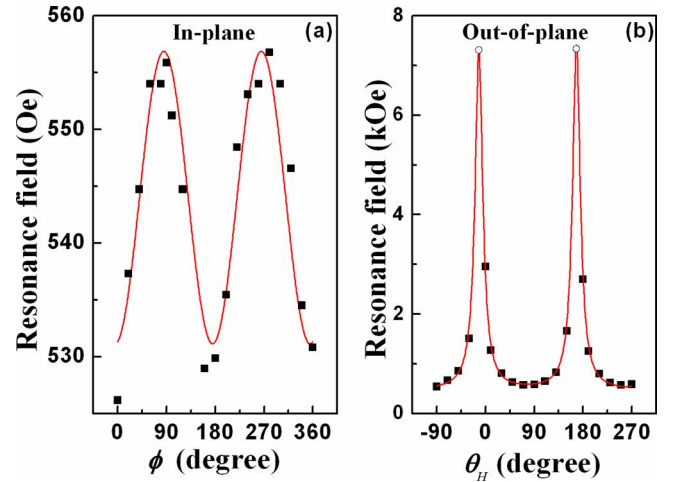


FIG. 3. (Color online) Angular dependencies of resonance fields of the FMR spectrum in both (a) the in-plane and (b) the out-of-plane configuration for the sample with the 20 Å Cr layers. The solid lines show the fitting using Eqs. (3) and (4). The resonant field at $\theta_H \approx 0^\circ$ and 180° is a singularity and cannot be reached in our measurements. The twofold result indicates the uniaxial anisotropic symmetry for the in-plane and the out of plane configuration as the applied field is rotated away from the easy axis.

$$\left(\frac{\omega^+}{\gamma} \right)^2 = \left[H_R^a \cos(\theta_H - \theta) - \left(4\pi M - \frac{2K_{\perp}}{M} \right) \cos 2\theta \right] \times \left[H_R^a \cos(\theta_H - \theta) - \left(4\pi M - \frac{2K_{\perp}}{M} \right) \cos^2 \theta - \frac{2K_{\parallel}}{M} \right], \quad (4)$$

where H_R^a represents the resonance field for the acoustic mode and $2K_{\parallel}/M$ and $2K_{\perp}/M$ are the effective in-plane uniaxial magnetic anisotropy field and the effective out-of-plane uniaxial anisotropy field. We first use Eq. (3) to fit the in-plane data and obtain the effective in-plane uniaxial magnetic anisotropy field $2K_{\parallel}/M$ of ~ 20 Oe and the demagnetization field $4\pi M$ of $\sim 2.1 \times 10^4$ Oe for the 20 Å Cr layer sample, as shown in Fig. 3(a). Next, we use the obtained parameters to describe our out-of-plane FMR data. Figure 3(b) reveals the measured and calculated resonant fields in the out-of-plane configuration. We realized that as the applied field moves away from the in-plane orientation, the magnetization does not change at an identical rate to the applied field. We calculate the equilibrium angle of magnetization by minimizing the free energy according to θ for different values of θ_H ; the results of which are shown in Fig. 4. The magnetization M immediately begins to seek the easy orientation as the magnetic field is tilted away from the direction normal to the sample surface (the resonant field at $\theta_H = 0^\circ$ is a “singularity” and cannot be reached). In contrast to the out-of-plane configuration, the resonant magnetic fields are sufficiently high enough to turn the magnetization vector M parallel to the applied magnetic field H in the in-plane orientations.

In addition to the acoustic branch of spin wave modes, we also observe a higher frequency FMR peak that could be referred to as the optical mode, as expected from Eq. (2). The acoustic and optical modes exist together in the spectrum for

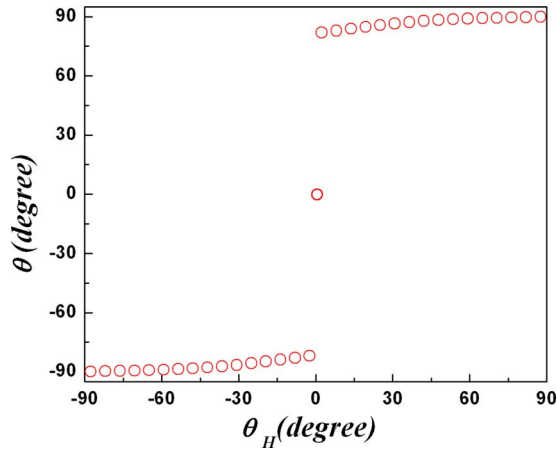


FIG. 4. (Color online) Equilibrium angle of the magnetization θ as a function of the angle of the applied field θ_H in the out-of-plane configuration ($\varphi=0^\circ$).

the multilayer system.^{10,11} When they are close enough, the FMR lines will partially overlap and form asymmetric absorption peaks. Figure 5 shows such a typical FMR spectrum: the broad feature at the high field side of the acoustic spin wave resonance mode can be deconvoluted to yield a weak absorption line that is attributed to the optical mode. The optical mode disturbs the main resonance line and introduces an additional contribution of the FMR linewidth and an asymmetric line shape. The acoustic and optical spin wave modes describe the interlayer coupled precession of magnetization vectors, as illustrated in the inset of Fig. 5. We could understand the nature of the interlayer interactions by estimating the differences in resonance field between the acoustic and optical modes.

B. Spin dynamical optical mode and magnetic interlayer coupling

Figure 6 shows the angular dependences of resonance fields including the acoustic and optical modes in both (a) the in-plane and (b) the out-of-plane configurations for the sample with 20 Å Cr layers. Similar to the acoustic mode, the optical mode also shows the twofold geometry due to the

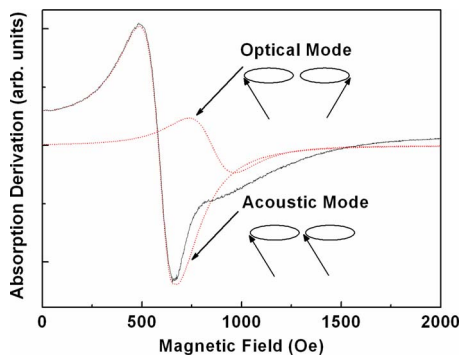


FIG. 5. (Color online) A typical FMR spectrum in the sample with the 20 Å Cr layers. The red dashed lines show the deconvolution of the spectrum, indicating acoustic and optical modes. The inset of the figure shows the schematic of these two modes. While the in-phase precession refers to the acoustic spin wave resonance, the out-of-phase precession is attributed to the optical spin wave resonance.

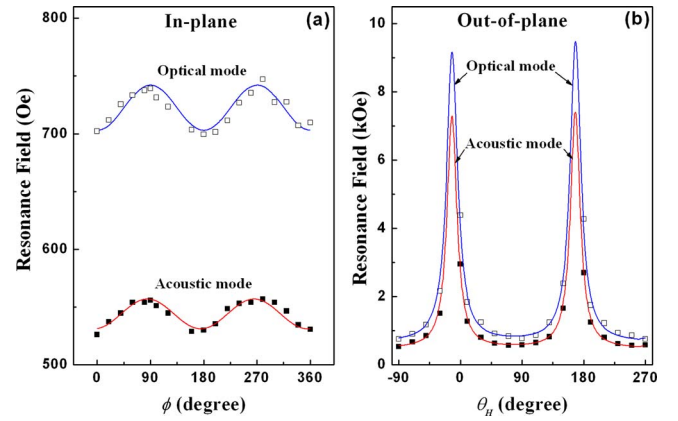


FIG. 6. (Color online) Angular dependence of resonance fields of the acoustic and optical modes in both (a) the in-plane and (b) the out-of-plane configuration for the sample with 20 Å Cr layers. The solid lines of the optical mode represent the fitting results using Eqs. (5) and (6).

uniaxial anisotropy contribution. Furthermore, we notice that the differences in resonant field of the acoustic and optical modes ($\Delta H=H^o-H^a$) show different behaviors in the in-plane and the out-of-plane configurations. We derive the expression of the resonant field for the optical branch from Eq. (2) by including the interlayer interactions, which takes forms of

$$\left(\frac{\omega^-}{\gamma}\right)^2 = \left(H_R^o - \frac{2K_{\parallel}}{M} \cos 2\varphi - J_{\text{eff}}\right) \left(H_R^o + 4\pi M - \frac{2K_{\perp}}{M} + \frac{2K_{\parallel}}{M} \sin^2 \varphi - J_{\text{eff}}\right), \quad (5)$$

$$\left(\frac{\omega^-}{\gamma}\right)^2 = \left[H_R^a \cos(\theta_H - \theta) - \left(4\pi M - \frac{2K_{\perp}}{M}\right) \cos 2\theta - J_{\text{eff}} \right] \left[H_R^a \cos(\theta_H - \theta) - \left(4\pi M - \frac{2K_{\perp}}{M}\right) \cos^2 \theta - \frac{2K_{\parallel}}{M} - J_{\text{eff}} \right], \quad (6)$$

where H_R^o represents the resonant field for optical mode and $J_{\text{eff}} = -2J_{\text{inter}}/dM$ (d is the thickness of a single FM layer). In the FMR measurement, since $\omega^+ = \omega^-$, the relation between H_R^o and H_R^a can be calculated by combining Eqs. (3) and (4) with Eqs. (5) and (6). We finally have

$$H^o = H^a + \frac{J_{\text{eff}}}{\cos(\theta_H - \theta)} \quad (\text{out of plane}), \quad (7)$$

$$H^o = H^a + J_{\text{eff}} \quad (\text{in plane}). \quad (8)$$

The magnetic interlayer coupling is determined by the J_{inter} : the adjacent two FM layers in the sample are FM coupled with a positive J_{inter} but are AFM coupled with a negative J_{inter} .³³ In turn, a positive J_{eff} represents the AFM coupled FM layers (since the J_{eff} is defined as $-2J_{\text{inter}}/dM$). For the data shown in Fig. 6, we obtain an interlayer coupling constant, J_{eff} as of ~ 179.8 Oe, by fitting the optical branch data using Eqs. (7) and (8).

TABLE I. Interlayer coupling constant J_{eff} and the effective in-plane uniaxial magnetic anisotropy $2K_{\parallel}/M$ for samples with different Cr layer thicknesses.

Cr layer thickness (Å)	J_{eff} (Oe)	$2K_{\parallel}/M$ (Oe)
4	120.1 ± 4.9	13.9 ± 1.3
10	160.3 ± 2.2	14.3 ± 0.4
20	179.8 ± 6.8	14.7 ± 0.2
30	280.4 ± 4.3	16.6 ± 1.1
40	220.2 ± 2.9	36.0 ± 3.2

Further, in order to understand how the interlayer spacing affects the interactions between FM layers, we calculated the J_{eff} according to FMR spectra in a series of FeCoB/Cr/FeCoB multilayers with different thicknesses of the Cr layers. The values are shown in Table I. We realize that the adjacent two FM layers are all antiferromagnetically coupled in our sample since the values for J_{eff} are all positive. This is consistent with our original assumption: $\varphi_2 = -\varphi_1$. Moreover, we find that the interlayer coupling constant J_{eff} does not increase monotonically with the Cr layer thickness but shows an oscillatory behavior. The result can be explained by the quantum interference³⁴ between adjacent FM layers. Because of the reflection of Bloch wave on interfaces of FM/AFM layers, multiple interferences could occur in Cr spacers and a phase shift is expected for the itinerant electron wave function. The phase shift varies with different interlayer Cr thicknesses and therefore changes the density of itinerant electron states. Since the density of the itinerant electron states determines the interlayer coupling strength, we could see an oscillatory change in J_{eff} as we increase the thickness of the spacing Cr layer.

It is important to note that the magnetic parameters are also affected in response to the change in the interlayer coupling between neighboring FM layers. Table I shows the in-plane uniaxial magnetic anisotropy constant for samples with different Cr layer thicknesses from our FMR measurements. We observe that the in-plane uniaxial magnetic anisotropy increases monotonically as the Cr layer thickness is changed from 4 to 40 Å. This is attributed to the redistribution of the magnetic moments in the FM layers by the interlayer interactions. Moreover, we find that the out-of-plane uniaxial anisotropy $2K_{\perp}/M$ is directly related to the change in the interlayer coupling strength. As shown in Fig. 7, an oscillatory change in the out-of-plane uniaxial anisotropy $2K_{\perp}/M$ can be clearly observed as we change the thickness of the Cr spacing layer in the FeCoB/Cr/FeCoB multilayers. This could result from the effective modification of surface and interface anisotropy energy as we change the thickness of the spacing layer. An effective magnetic anisotropy in the perpendicular direction is introduced into the free magnetic energy density due to the interface and surface contributions, which is directly related to the interlayer interactions and therefore shows an oscillatory change as a result of increasing the thickness of the spacing layers. It is important to mention that we could use the interlayer coupling between the FM layers as an additional means to optimize the mag-

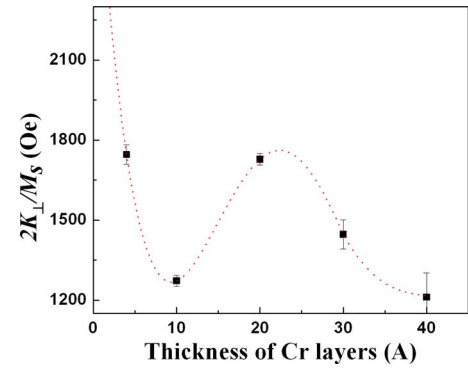


FIG. 7. (Color online) Dependence of the out-of-plane effective anisotropy $2K_{\perp}/M$ on the Cr layer thickness. The oscillatory behavior indicates the connection with the interlayer coupling. The dashed line is only meant to guide the eyes.

netic anisotropy parameters in multilayer magnetic structures (simply by tuning the thickness of the spacing AFM layer.)

C. Spin wave resonance linewidth and relaxation

Finally, we investigate the magnetic relaxation dynamics (damping) of our samples, which is a parameter of paramount importance for rf/microwave applications such as microwave band stop filters. Large FMR linewidth leads to a reduced quality factor and increased insertion loss, which are among the major problems associated with the microwave band stop filters. So far, significant progress has been made regarding the understanding of the FMR behavior of exchange-coupled FM/AFM bilayers and the physical contribution to the FMR linewidth. However, relatively less amount of work is done on the exchange coupled FM/AFM/FM trilayers, and their microwave performances are not well understood. We measured the FMR linewidth, peak to peak field separation ΔH_{pp} , as a function of in-plane applied field angle. The intrinsic FMR linewidth can be derived from the free energy density F by the relation³⁵

$$\Delta H_{\text{in}} = \frac{2}{\sqrt{3}} \frac{1}{\left| \frac{\partial \omega}{\partial H_{\text{res}}} \right|} \frac{\alpha \gamma}{M} \left(\frac{\partial^2 F}{\partial \theta^2} + \frac{1}{\sin^2 \theta} \frac{\partial^2 F}{\partial \varphi^2} \right), \quad (9)$$

where α is a Gilbert damping parameter which determines how fast the energy of the magnetization precession is dissipated from the system. Figure 8 illustrates the FMR linewidth as a function of the in-plane angle ϕ between the applied field and the easy axis in the sample with 20 Å Cr layers. The solid line shows a fit by using Eq. (9). We calculate the Gilbert damping parameter α according to the above equation and obtained $\alpha = 0.0101 \pm 0.0005$. Moreover, we find that the FMR linewidth and therefore the Gilbert damping could also be optimized by varying the thicknesses of Cr layers.

Figure 9 shows the FMR linewidth and α as a function of Cr layer thickness for the FeCoB/Cr/FeCoB multilayer samples. The magnetic field is applied along their in-plane easy axis direction. As we can see in Fig. 8, there is an oscillation for both the damping constant α and FMR linewidth which is consistent with the variation in interlayer con-

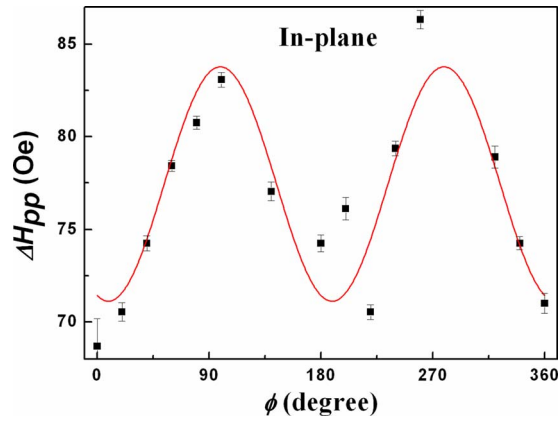


FIG. 8. (Color online) FMR linewidth as a function of the in-plane applied field angle ϕ for the sample with 20 Å Cr layers. The solid red line shows the fitting result using Eq. (9).

stant J_{eff} . The result suggests that the interlayer coupling plays an important role in determining the magnetization relaxation dynamics in multilayer materials. As discussed above, itinerant electrons are confined in the adjacent FM layers and they introduce an extra exchange interaction. An extra relaxation torque will be added into the system and contributes to the FMR linewidth in the multilayer structures.³⁶ We expect an oscillatory change in the FMR linewidth as we increase the thickness of the spacing layer since the exchange interaction is determined by the density of itinerant electron states. Thus, compared with single and bilayer structures, multilayer structures show an additional degree of freedom to control the magnetic anisotropy and relaxation properties (simply by varying the interlayer coupling between the neighboring FM layers) in addition to a higher effective magnetization.

IV. CONCLUSION

In summary, we investigated the magnetic dynamic properties including magnetic anisotropies, acoustic and optical modes, interlayer coupling, and magnetization damping

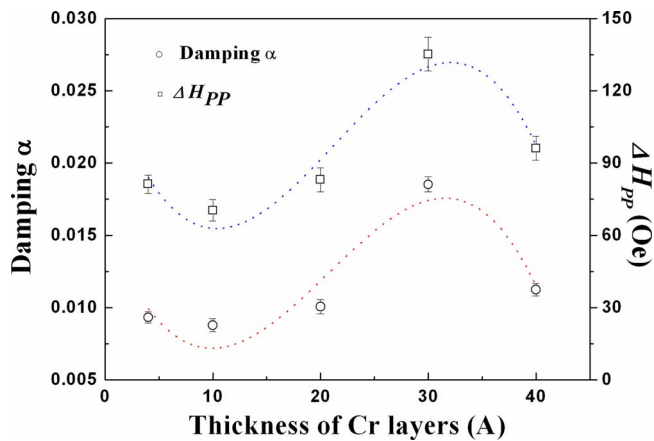


FIG. 9. (Color online) FMR linewidth and magnetization damping constant α as a function of the thickness of Cr layers. Both of them show the oscillatory change, which is consistent with the variation in interlayer constant J_{eff} . This suggests that the interlayer coupling plays an important role in determining the magnetization relaxation dynamics in multilayer materials. The dashed line is only meant to guide the eyes.

of multilayer FeCoB/Cr/FeCoB films. The FMR measurements were carried out for samples with the AFM Cr layer thicknesses varying from 4 to 40 Å. We identify both the acoustic and optical branches in the spin wave resonance spectra. The magnetic layers in our samples are shown to be coupled antiferromagnetically by the effective interlayer coupling constant J_{eff} . We determine the uniaxial in-plane anisotropy parameter $2K_{\parallel}/M$ and the out-of-plane anisotropy $2K_{\perp}/M$ for samples with different Cr interlayer thicknesses. Moreover, magnetization relaxation is estimated by analyzing the FMR linewidth as a function of the angle between the external field and easy axis and as a function of the Cr layer thickness. Further, we reveal that the out-of-plane magnetic anisotropy and the magnetization damping show an oscillatory change with increasing interlayer spacing, similar to the interlayer coupling constant, while the in-plane magnetic anisotropy increases monotonically. Our results suggest that we could use the interlayer coupling between the FM layers as an additional means to optimize the magnetic anisotropy and magnetic relaxation properties in multilayer magnetic structures, which is important for applications in high frequency devices.

ACKNOWLEDGMENTS

We are grateful to Dr. Philip Stallworth for illuminating discussions. We also thank Professor Steve Greenbaum for allowing us to use his EPR/FMR facilities. This work is supported in part by the Petroleum Research Fund and PSC-CUNY award.

- ¹M. Yamaguchi, S. Arakawa, H. Ohzeki, Y. Hayashi, and K. I. Arai, *IEEE Trans. Magn.* **28**, 3015 (1992).
- ²A. M. Crawford, D. Gardner, and S. X. Wang, *IEEE Trans. Magn.* **38**, 3168 (2002).
- ³B. Kuanr, Z. Celinski, and R. E. Camley, *Appl. Phys. Lett.* **83**, 3969 (2003).
- ⁴E. Šimánek and B. Heinrich, *Phys. Rev. B* **67**, 144418 (2003).
- ⁵B. Viala, A. S. Royet, R. Cuchet, M. Aid, P. Gaud, O. Valls, M. Ledieu, and O. Acher, *IEEE Trans. Magn.* **40**, 1999 (2004).
- ⁶B. Kuanr, D. L. Marvin, T. M. Christensen, R. E. Camley, and Z. Celinski, *Appl. Phys. Lett.* **87**, 222506 (2005).
- ⁷M. Gruyters and D. Riegel, *Phys. Rev. B* **63**, 052401 (2000).
- ⁸P. Miltényi, M. Gierlings, J. Keller, B. Beschoten, and G. Güntherodt, *Appl. Phys. Lett.* **84**, 4224 (2000).
- ⁹M. Ali, C. H. Marrows, M. Al-Jawad, and B. J. Hickey, *Phys. Rev. B* **68**, 214420 (2003).
- ¹⁰P. Blomqvist, K. M. Krishnan, and E. Girt, *J. Appl. Phys.* **95**, 8487 (2004).
- ¹¹J. Nogués, *Phys. Rev. B* **61**, 1315 (2000).
- ¹²K. Nakamura, A. J. Freeman, and D. S. Wang, *Phys. Rev. B* **65**, 012402 (2001).
- ¹³M. Grimsditch, A. Hoffmann, P. Vavassori, H. Shi, and D. Lederman, *Phys. Rev. Lett.* **90**, 257201 (2003).
- ¹⁴S. M. Zhou and C. L. Chien, *Phys. Rev. B* **63**, 104406 (2001).
- ¹⁵S. X. Wang, N. X. Sun, M. Yamaguchi, and S. Yabukami, *Nature (London)* **407**, 150 (2000); C. Pettiford, A. Zeltser, S. Z. D. Yoon, V. G. Harri, C. Vittoria, and N. X. Sun, *J. Appl. Phys.* **99**, 08C901 (2006).
- ¹⁶Y. H. Ren, C. Wu, G. Yu, C. Pettiford, and N. X. Sun, *J. Appl. Phys.* **105**, 073910 (2009); C. Wu, S. Greenbaum, C. Pettiford, N. X. Sun, and Y. H. Ren, *ibid.* **103**, 07B525 (2008).
- ¹⁷C. Bellouard, J. Faure-Vincent, C. Tiusan, F. Montaigne, M. Hehn, V. Leiner, H. Fritzsche, and M. Gierlings, *Phys. Rev. B* **78**, 134429 (2008).
- ¹⁸D. Aernout, M. Rots, and J. Meerschaert, *Phys. Rev. B* **77**, 174413 (2008).
- ¹⁹S. Blomeier, P. Candeloro, B. Hillebrands, B. Reuscher, A. Brodyanski, and M. Kopnarski, *Phys. Rev. B* **74**, 184405 (2006).
- ²⁰Z. Celinski and B. Heinrich, *J. Magn. Magn. Mater.* **99**, L25 (1991).
- ²¹B. Heinrich, J. F. Cochran, M. Kowalewski, J. Kirschner, Z. Celinski, A.

- S. Arrott, and K. Myrtle, *Phys. Rev. B* **44**, 9348 (1991).
- ²²M. E. Filipkowski, J. J. Krebs, G. A. Prinz, and C. J. Gutierrez, *Phys. Rev. Lett.* **75**, 1847 (1995).
- ²³W. E. Bailey, S. E. Russek, X. G. Zhang, and W. H. Butler, *Phys. Rev. B* **72**, 012409 (2005).
- ²⁴D. Tripathy, A. O. Adeyeye, and S. Shannigrahi, *Phys. Rev. B* **75**, 012403 (2007).
- ²⁵P. M. Haney, D. Waldron, R. A. Duine, A. S. Núñez, H. Guo, and A. H. MacDonald, *Phys. Rev. B* **75**, 174428 (2007).
- ²⁶N. Planckaert, C. L'abbé, B. Croonenborghs, R. Callens, B. Laenens, A. Vantomme, and J. Meersschant, *Phys. Rev. B* **78**, 144424 (2008).
- ²⁷B. Heinrich, Y. Tserkovnyaki, G. Woltersdorf, A. Brataas, R. Urban, and G. E. W. Bauer, *Phys. Rev. Lett.* **90**, 187601 (2003).
- ²⁸B. Heinrich, Z. Celinski, J. F. Cochran, W. B. Muir, J. Rudd, Q. M. Zhong, A. S. Arrott, K. Myrtle, and J. Kirschner, *Phys. Rev. Lett.* **64**, 673 (1990).
- ²⁹J. J. Krebs, P. Lubitz, A. Chaiken, and G. A. Prinz, *Phys. Rev. Lett.* **63**, 1645 (1989).
- ³⁰A. Brambilla, P. Biagioni, M. Portalupi, M. Zani, M. Finazzi, L. Duò, P. Vavassori, R. Bertacco, and F. Ciccacci, *Phys. Rev. B* **72**, 174402 (2005).
- ³¹T. J. Klemmer, K. A. Ellis, L. H. Chen, B. van Dover, and S. Jin, *J. Appl. Phys.* **87**, 830 (2000).
- ³²J. Smit and H. G. Beljers, *Philips Res. Rep.* **10**, 113 (1955).
- ³³J. Lindner and K. Baberschke, *J. Phys.: Condens. Matter* **15**, S465 (2003).
- ³⁴P. Bruno, *Phys. Rev. B* **52**, 411 (1995).
- ³⁵H. Suhl, *Phys. Rev.* **97**, 555 (1955).
- ³⁶R. Urban, G. Woltersdorf, and B. Heinrich, *Phys. Rev. Lett.* **87**, 217204 (2001).